Arginase 2 attenuates ulcerative colitis by antioxidant effects of spermidine

今津, 愛介

Arginase 2 attenuates ulcerative colitis by antioxidant effects of spermidine

Arginase 2, spermidine in UC

Noriyuki Imazu[1)], Takehiro Torisu[1)], Akihito Yokote[1)], Junji Umeno[1)], Keisuke Kawasaki[1)], Shin Fujioka[2)], Yuichi Matsuno[1)], Tomohiro Nagasue[1)], Shinichiro Kawatoko[1)], Tomohiko Moriyama[3)], Tomoki Nitahata[1)], Yushi Uchida[1)], Seishi Aihara[1)], Yoshiaki Taniguchi[4)], Yoshinao Oda[4)], Takanari Kitazono[1)]

1) Department of Medicine and Clinical Science, Graduate School of Medical Sciences, Kyushu University, Fukuoka, Japan
2) Department of Endoscopic Diagnostics and Therapeutics, Kyushu University Hospital, Fukuoka, Japan
3) Department of International Medical Department, Kyushu University Hospital, Fukuoka, Japan
4) Department of Anatomic Pathology, Graduate School of Medical Science, Kyushu University, Fukuoka, Japan

Corresponding author: Takehiro Torisu, MD., Ph.D.
Department of Medicine and Clinical Science, Graduate School of Medical Sciences, Kyushu University, Maidashi 3-1-1, Higashi-ku, Fukuoka 812-8582, Japan

Telephone: +81-92-642-5261; fax: +81-92-642-5273

E-mail: torisu.takehiro.437@m.kyushu-u.ac.jp

Word counts

Abstract: 211 words; main text: 5474 words; references: 47; figures: 6.

Abstract

Background:

Spermidine suppress oxidative stress and is involved in various disease pathogenesis including ulcerative colitis (UC). Arginase 2 (ARG2) plays a central role in the synthesis of spermidine. This study aimed to clarify the effect of endogenously produced spermidine on colitis.

Methods:

The physiological role of ARG2 and spermidine was investigated using *Arg2*-deficient mice with reduced spermidine. Immunohistochemical staining of the rectum was used to analyze ARG2 expression and spermidine levels in healthy controls and UC patients.

Results:

In mice with dextran sulfate sodium induced colitis, ARG2 and spermidine levels were increased in the rectal epithelium. Spermidine protects colonic epithelial cells from oxidative stress and *Arg2* knockdown cells reduced antioxidant activity. Organoids cultured from the small intestine and colon of *Arg2*-deficient mice both were more susceptible to oxidative stress. Colitis was exacerbated in *Arg2*-deficient mice compared to wild-type mice. Supplementation with spermidine result in comparable severity of colitis in both wild-type and *Arg2*-deficient mice. In the active phase of UC, rectal ARG2 expression and spermidine accumulation were increased compared to remission.

ARG2 and spermidine levels were similar in healthy controls and UC remission patients.

Conclusions:

ARG2 produces spermidine endogenously in the intestinal epithelium and has a palliative effect on ulcerative colitis. ARG2 and spermidine are potential novel therapeutic targets for UC.

Keywords: ulcerative colitis, arginase 2, spermidine, antioxidant effect

Abbreviations

ARG2; arginase 2

DAPI; 4,6-diamino-2-phenylindole

DSS; dextran sulfate sodium

GCL; glutamate-cysteine ligase

GCLC; glutamate-cysteine ligase catalytic subunit

GCLM; glutamate-cysteine ligase modifier subunit

HDAC2; histone deacetylase 2

HE; hematoxylin–eosin

HO-1; heme oxygenase-1

H_2O_2; hydrogen peroxide

IBD; inflammatory bowel disease

KO; knockout

LPS; lipopolysaccharide

NQO1; nicotinamide quinone oxidoreductase 1

NRF2; nuclear factor erythroid 2-related factor 2

PCR; polymerase chain reaction

ROS; reactive oxygen species

SPD; spermidine

TNFα; tumor necrosis factor-α

TXNR; thioredoxin reductase 1

UC; ulcerative colitis

Introduction

Inflammatory bowel disease (IBD) is a chronic, idiopathic, inflammatory disease comprising ulcerative colitis (UC) and Crohn's disease (CD)[1]. The incidence of IBD exceeds 0.3%, and more than 5 million people are affected worldwide [2]. UC is characterized by a complex interplay of immune mediators. Current treatment approaches, such as corticosteroids, immunomodulators, janus kinase inhibitors, and various biologic agents, have been developed to treat UC. However, treatment resistance and failure continue to be major challenges [3]. The management of severe and opportunistic infections is crucial because of immunosuppression in therapy [4]. Most current therapies affect systemic immunity[5, 6]. Therefore, a novel therapy with protective effects on the epithelium rather than immunosuppressive properties is required.

Polyamines are linear aliphatic hydrocarbons consisting of three or more polymerized primary amino acids, which include putrescine, spermidine (SPD), and spermine [7]. The urea cycle is one of the polyamine production pathways in which ornithine is produced from L-arginine catalyzed by arginase and then converted to putrescine, SPD, and spermine [8]. SPD has been studied for its physiological activity, which includes suppressing oxidative stress, promoting autophagy, and extending the cellular lifespan [9]. In the intestinal mucosa, SPD contributes to wound healing, epithelial repair, maintenance of epithelial barrier function, and epithelial cell proliferation [10]. Elevated SPD concentrations are found in the colonic epithelium in patients with UC [11] [12].

Additionally, in spermine oxidase (an enzyme that produces SPD) knockout (KO) mice, dextran sulfate sodium (DSS)-induced enteritis worsens, but SPD supplementation improves this disease [13]. Furthermore, putrescine produced by the intestinal microbiota is absorbed into the epithelium and produces SPD, which alleviates experimental colitis [14].

Polyamines are produced from L-arginine (L-Arg) by catalysis with arginase. Arginase exists in two subtypes of arginase 1, which is found in the cytoplasm, and arginase 2 (ARG2), which is a mitochondrial enzyme. ARG2 is predominantly expressed in the small intestine and colon [15] [16]. The relationship between L-Arg and inflammatory bowel disease has been the focus of research, and L-Arg supplementation is suggested as a possible method to improve intestinal inflammation [17] [18].

Despite previous research, the role of arginase and endogenous SPD in intestinal inflammation is not well understood. Therefore, this study aimed to examine the anti-inflammatory effects of SPD in the intestinal epithelium using *Arg2* KO mice or knockdown cell lines, which are necessary for SPD production.

Methods

Animals

Arg2 KO mice (*Arg2*^{tm1Weo}/J) of C57BL/6 background were purchased from the Jackson Laboratory, and heterozygous crosses were performed to generate wild-type (WT) and *Arg2* KO littermates. Female mice aged 8–12 weeks were used for the experiments and housed in specific pathogen-free conditions. All mouse experiments were conducted following the guidelines provided by the Guide for the Care and Use of Laboratory Animals of the National Institutes of Health. The protocol was approved by the Committee on the Ethics of Animal Experiments of the Kyushu University (approval numbers: A19-253-1, A21-092-2, and A23-097-0). The experiments were reported according to the ARRIVE guidelines.

Mouse model of DSS-induced colitis

Colitis was induced in the mice by administering 2.5% DSS (FUJIFILM Wako Pure Chemical Corporation, Osaka, Japan) orally for 5 consecutive days followed by drinking sterile water for 5 days. On the 10th day, the mice were euthanized under anesthesia by intraperitoneal injection of a combination of 0.3 mg/kg medetomidine hydrochloride, 5 mg/kg butorphanol tartrate, and 4 mg/kg midazolam. The SPD supplementation group received oral administration of 2.5% DSS along with 20mM SPD for 5days, followed by oral administration of 20mM SPD, and were euthanized on the 10th day following the same protocol. The stool consistency score was evaluated on the basis of previous reports[19] as follows: 0 (normal), 1 (semi-solid), 2 (loose to pasty), and 3 (diarrhea). This score was evaluated daily, and the cumulative score was calculated.

Cell lines and culture

Human colon cancer cell lines, HCT116 (RCB2979) and Caco-2 (RCB0988), were provided by RIKEN BRC through the National Bio-Resource Project of MEXT/AMED, Japan. The cells were cultivated in Dulbecco's modified Eagle medium containing 10% fetal bovine serum, 100 U/ml penicillin, and 100 mg/ml streptomycin (Nacalai Tesque, Kyoto, Japan). ARG2 expression was suppressed by short interfering RNA (siRNA)-mediated knockdown (L-009454-01-0010; Horizon Discovery, Cambridge, UK). HCT116 and Caco-2 cells were transfected with 10 nmol/L of the indicated siRNA using Dharmafect 1 transfection reagent (Horizon Discovery) as reported previously. [20]

Polyamine detection assay

HCT116 cells were transfected by control or *Arg2* siRNA for 24 h. The cells were then stimulated by 500 ng/ml lipopolysaccharide ([LPS] L-2630; Sigma-Aldrich, ST. Louis, Missouri, USA) or 50 ng/ml tumor necrosis factor-α ([TNFα] 201-18581; FUJIFILM Wako Pure Chemical Corporation) and incubated for 24 h. The medium was removed and stained with PolyamineRED (Funakoshi Co., Tokyo, Japan). The cells were fixed in 4% paraformaldehyde, stained with 4,6-diamino-2-phenylindole (DAPI), and observed under a fluorescence microscope (BZ-X700; Keyence, Osaka, Japan). Fluorescence intensity was analyzed using ImageJ software (National Institutes of Health, Bethesda, MD, USA).

Intracellular reactive oxygen species detection assay

HCT116 cells were transfected by control or *Arg2* siRNA for 24 h. Stimulation of 500 ng/ml LPS, 50 ng/ml TNFα, or 250 μM hydrogen peroxide (H_2O_2) was performed, and the cells were incubated for 24 h. We used the ROS (reactive oxygen species) Assay Kit - Highly Sensitive DCFH-DA- (Dojindo, Kumamoto, Japan) and Cellstain Hoechst 33342 solution (H342; Dojindo) according to a previous report [20]. Imaging was carried out using a BZ-X700 microscope (Keyence) and analysis was performed with ImageJ software.

Cell viability assay

HCT116 and Caco-2 cells were transfected with control or *Arg2* siRNA for 24 h. Subsequently, 800 μM and 1000 μM concentrations of H_2O_2 were administered to the HCT116 and Caco-2 cell medium, respectively, and cultured. After another 24 h of incubation in accordance with the manufacturer's protocol and a previous report [21], the absorbance at 450 nm was measured using the viable cell counting reagent SF (Nacalai Tesque).

Western blotting

Colon tissues in T-PER Tissue Protein Extraction Reagent (Thermo Fisher Scientific, Waltham, MA, USA) were homogenized using the TissueLyser (Qiagen, Venlo, Netherland) in accordance with the manufacturer's instructions. The cells were lysed in M-PER Mammalian Protein Extraction Reagent or N-PER Neuronal Protein Extraction Reagent (Thermo Fisher Scientific). Western blotting was performed as previously described. [22] The following primary antibodies were used for the analysis: mouse

anti-nuclear factor erythroid 2-related factor 2 (NRF2) monoclonal antibody (sc-365949; Santa Cruz Biotechnology, Dallas, TX, USA); rabbit anti-β-actin (ab8227; Abcam, Cambridge, UK); rabbit anti-arginase 2 antibody (#19324; Cell Signaling, Danvers, MA, USA); rabbit anti-heme oxygenase-1 (HO-1) antibody (10701-1-AP; Proteintech, Rosemont, IL, USA), rabbit anti-glutamate-cysteine ligase modifier subunit (GCLM) antibody (14241-1-AP; Proteintech), rabbit-thioredoxin reductase 1 (TXNR) antibody (11117-1-AP; Proteintech), rabbit anti-nicotinamide quinone oxidoreductase 1 (NQO1) antibody (11451-1-AP; Proteintech), and rabbit anti-histone deacetylase 2 antibody (ab75602; Abcam). The bands were detected using the Chemi-Lumi One Ultra kit (Nacalai Tesque) and a chemiluminescence imaging system (AE-9300 Ez capture MG; Atto, Tokyo, Japan). The density of each band was analyzed by ImageJ software (National Institutes of Health).

Real-time polymerase chain reaction

Total RNA was extracted from cells or tissues using the MAXWELL®16 LEV simplyRNA tissue kit (Promega, Madison, WI, USA) in accordance with the manufacturer's instructions. RNA concentrations were measured with the Qubit Fluorometer and Qubit RNA BR Assay Kit (Thermo Fisher Scientific). Complementary DNA was synthesized from 1 μg of total RNA with the PrimeScript RT Reagent kit (Takara Bio, Kusatsu, Japan). Real-time polymerase chain reaction (PCR) was performed using TB Green Premix Ex Taq™II (Takara Bio) and the Applied Biosystems QuantStudio 3 instrument (Thermo Fisher Scientific). The expression levels of each gene were calculated relative to the internal control.

Primer sequences were purchased from Takara Bio and were as follows: human ß-actin

(HA067803), human *Arg2* (HA144573), human *HO-1* (HA109356), human *GCLM* (HA328417), human *TXNR* (HA361942), human *NQO1* (HA354344), mouse ß-actin (MA050368), and mouse *Arg2* (MA234009).

Histological examination and immunostaining

Colon tissues were fixed in 4% paraformaldehyde and embedded in paraffin. The paraffin-embedded colon blocks were cut into 4-μm sections and subjected to hematoxylin–eosin (HE) staining. In the histological evaluation, the inflammation score, ulceration score, hyperplasia score, and disease area score were each evaluated on a 3-point scale, resulting in a total of 12 points [23].

To perform immunohistochemistry, colon tissue was removed from paraformaldehyde, sucrose-substituted, and embedded in Tissue Tek Optimal Cutting Temperature Compound (Sakura Finetek Japan, Tokyo, Japan). The frozen blocks were cut into 4-μm slices. The primary antibodies were rabbit anti-ARG2 antibody (bs11397-R; Bioss, Boston, MA, USA) and rabbit anti-SPD polyclonal antibody (ab7318; Abcam), and the secondary antibody was Alexa 488-conjugated goat anti-rabbit IgG (A11008; Life Technologies, Carlsbad, CA, USA). [24] After counterstaining with DAPI, images were obtained by a fluorescence microscope (BZ-X700; Keyence). The obtained images were analyzed using ImageJ software (National Institutes of Health).

Organoid culture and analysis

Organoid culture from the mouse intestine was performed as previously described[25]. In brief, the crypts were collected from the mouse small intestine and colon using

Gentle Cell Dissociation Reagent (Stemcell Technologies, Vancouver, Canada). The organoids mixed with Corning Matrigel Matrix (Corning, Corning, NY, USA) were seeded in a 24-well multiwell plate, and a complete medium (IntestiCult Organoid Growth Medium; Stemcell Technologies) was added. Passages were performed 7–10 days after culture and used for experiments.

The organoids were exposed to 500 μM H_2O_2 for 24 h. The viability of the organoids was evaluated by fluorescence observation using the Cyto 3D Live-Dead Assay Kit (TheWell Bioscience, North Brunswick, NJ, USA).

Statistical analysis

Values are shown as the mean ± standard error of the mean. Statistical analyses were conducted using JMP 16 software (SAS Institute, Cary, NC, USA).

Results

Stimulation of cell lines and induction of colitis via DSS administration in mice enhance SPD and ARG2 expression

To evaluate the accumulation of polyamines and expression of ARG2 in the intestinal epithelium during inflammation, we first stimulated a human colon cancer-derived cell line (HCT116) with LPS and TNFα. We found an elevation in polyamine levels with LPS and TNFα stimulation compared with controls (Figure 1A and B). In WT mice, DSS colitis was induced, and immunostaining of colonic epithelial tissue using an anti-SPD fluorescent antibody showed considerably higher SPD accumulation in the DSS colitis group than in the control group (Figure 1C and D). Our subsequent analysis of ARG2 protein expression in the HCT116 cell line showed that ARG2 expression increased in a H_2O_2 concentration-dependent manner (Figure 1E). Furthermore, *Arg2* mRNA transcription was enhanced when the cell line was subjected to H_2O_2 as oxidative stress (Figure 1F). Immunofluorescence staining of intestinal epithelial tissues from DSS colitis mice using anti-ARG2 antibody showed significantly increased ARG2 protein expression (Figure 1G and H). We also observed increased ARG2 protein expression extracted from intestinal tissue (Figure 1I). These findings suggest that ARG2 expression is elevated in colitis, indicating an augmented production of SPD originating from intestinal epithelial cells.

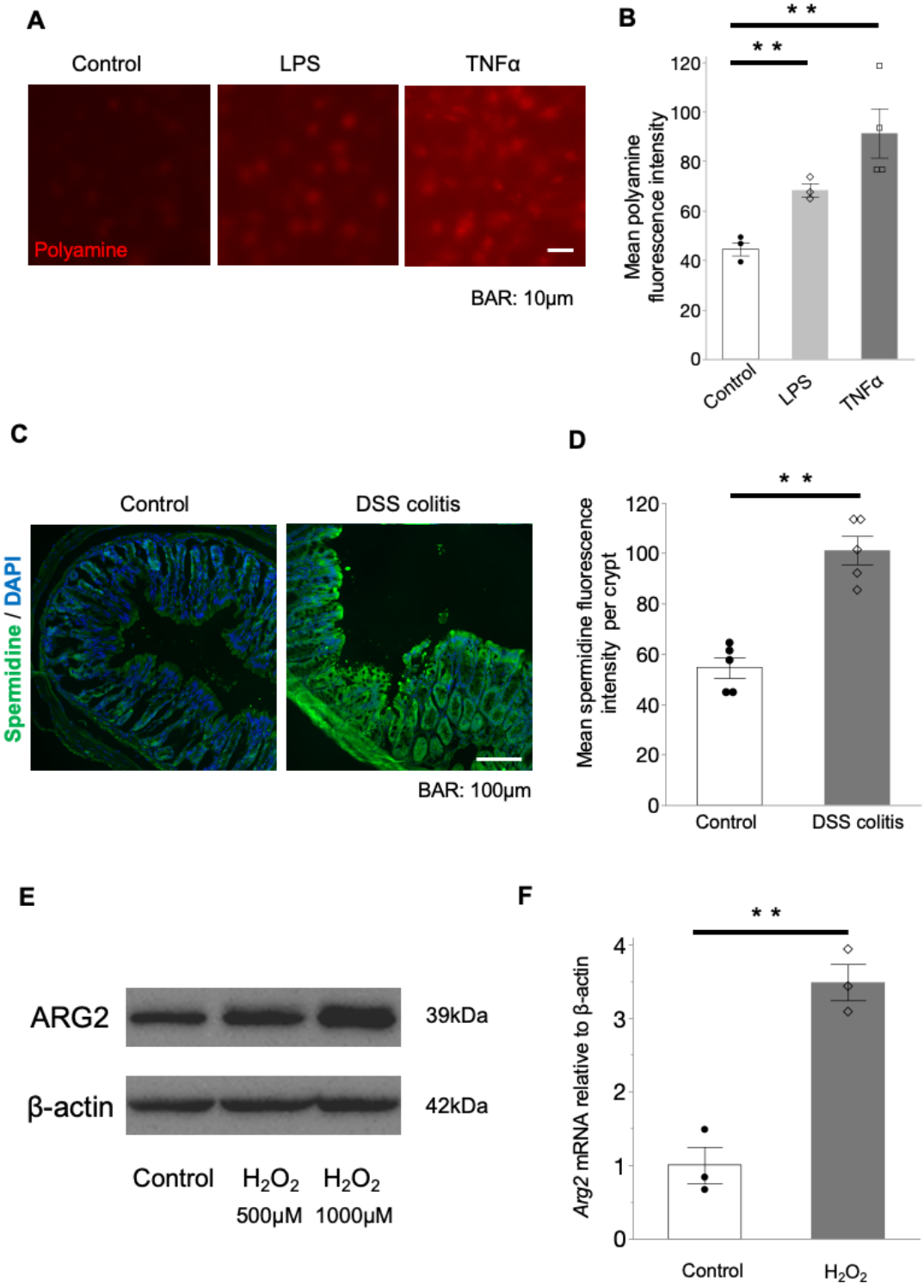
A
Control
LPS
TNFα
Polyamine
BAR: 10μm
B
Mean polyamine fluorescence intensity
120
100
80
60
40
20
0
Control
LPS
TNFα
C
Control
DSS colitis
Spermidine / DAPI
BAR: 100μm
D
Mean spermidine fluorescence intensity per crypt
120
100
80
60
40
20
0
Control
DSS colitis
E
ARG2
39kDa
β-actin
42kDa
Control
H2O2 500μM
H2O2 1000μM
F
Arg2 mRNA relative to β-actin
4
3
2
1
0
Control
H2O2

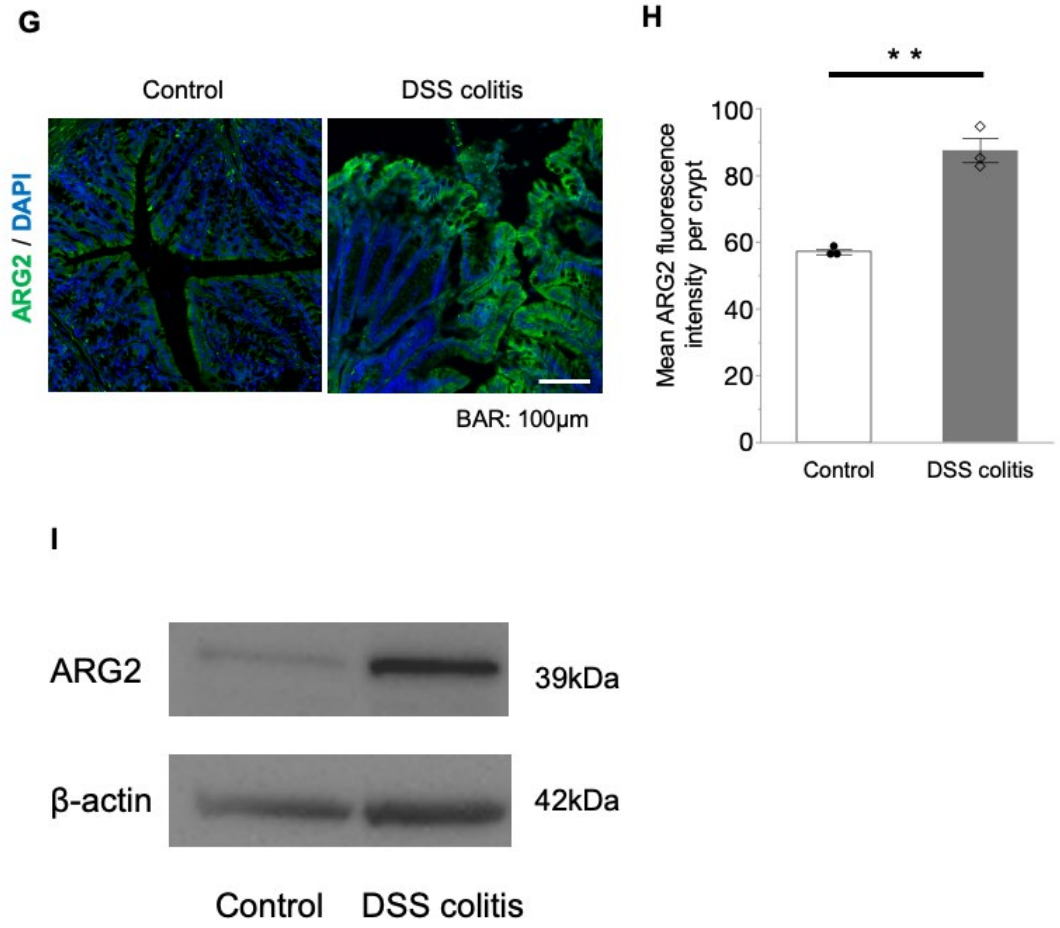

303

304 **Fig. 1 Accumulation of spermidine is enhanced in colonic epithelium during**

305 **inflammation.**

306 **A** Fluorescent imaging of polyamine in HCT116 cells treated with LPS (500 ng/ml) and

307 TNFα (50 ng/ml) for 24 h. Bar = 10 μm.

308 **B** Mean fluorescence intensity shows that polyamine levels were increased after

309 stimulation with LPS and TNFα (n = 3 in each group).

310 **C** Immunohistochemical staining with anti-SPD antibody was performed in the distal

311 colon of mice with and without DSS colitis. Bar = 100 μm.

312 **D** The accumulation of SPD was evaluated by fluorescence intensity in each of 15

crypts (n = 5 in each group).

E Western blotting analysis of ARG2 following H_2O_2 stimulation at the indicated concentrations for 24 h. ß-actin is shown as the loading control.

F Real-time PCR analysis shows that *Arg2* mRNA expression was increased by stimulation with H_2O_2 (1000 μM) for 12 h.

G Representative images of immunohistochemical staining of ARG2 for the distal colon of mice with and without DSS colitis. Bar = 100 μm.

H ARG2 protein expression was evaluated by averaging the fluorescence intensity in each of 15 crypts (n = 3 in each group).

I Western blotting analysis of ARG2 protein levels in the distal colon of control and DSS colitis.

The results are expressed as the mean ± standard error. The unpaired t test was used for analysis. *P < 0.05 and **P < 0.01. Abbreviations: DAPI; 4,6-diamino-2-phenylindole, DSS; dextran sulfate sodium, LPS; lipopolysaccharide, SPD; spermidine, TNFα; tumor necrosis factor-α.

SPD produces antioxidant effects via upregulation of NRF2-related pathways, inhibiting ROS production and protecting cells from oxidative stress

To determine the role of SPD, the HCT116 cell line was cultured with SPD, and the antioxidant pathway was investigated. We found upregulation of mRNA expression of *HO-1*, *GCLM*, *TXNR*, and *NQO1*, all of which are transcription factor NRF2-related pathways (Figure 2A). Furthermore, protein extraction and analysis showed that HO-1, GCLM, and TXNR protein levels were upregulated (Figure 2B). We then extracted proteins from cell nuclei and observed an increase in NRF2 protein levels (Figure 2C

and D). This finding indicates that SPD enhances the transcription of antioxidant genes and protein expression by promoting the transfer of NRF2 into the nucleus.

To assess the antioxidant effect of SPD, we exposed HCT116 cells to various stimuli (LPS, TNFα, and H_2O_2) and measured the production of ROS (reactive oxygen species) in the presence or absence of SPD. We found that SPD significantly inhibited ROS production in all stimuli (Figure 2E, F). Furthermore, we evaluated the viability of HCT116 cells under oxidative stress by inducing cell death with H_2O_2. We observed that SPD suppressed cell death compared with that in the control group (Figure 2G). These findings suggest that SPD has protective effects against oxidative stress.

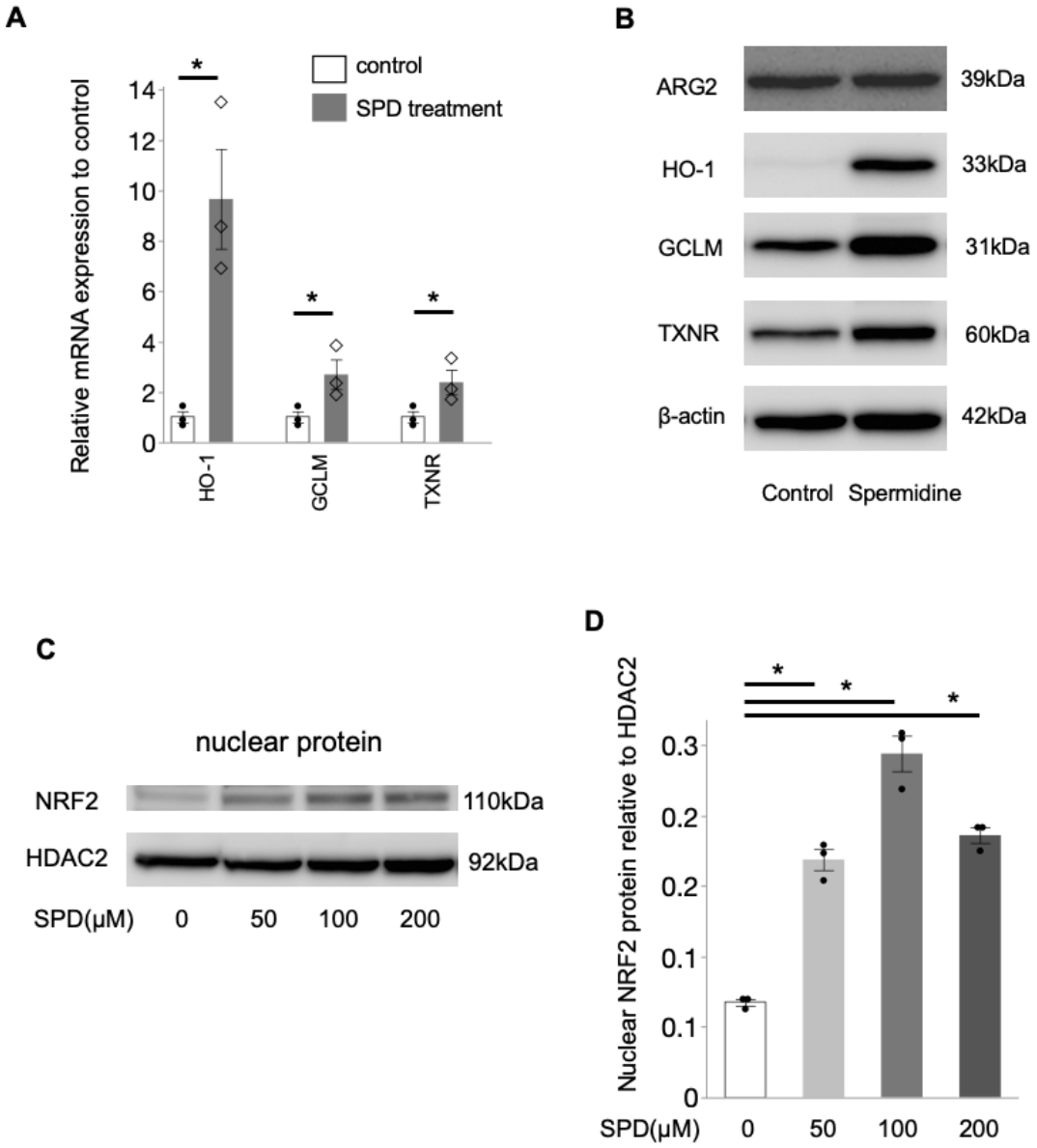
A
control
SPD treatment
Relative mRNA expression to control
14
12
10
8
6
4
2
0
*
*
*
HO-1
GCLM
TXNR
B
ARG2
39kDa
HO-1
33kDa
GCLM
31kDa
TXNR
60kDa
β-actin
42kDa
Control
Spermidine
C
nuclear protein
NRF2
110kDa
HDAC2
92kDa
SPD(μM) 0 50 100 200
D
Nuclear NRF2 protein relative to HDAC2
0.3
0.2
0.2
0.1
0.1
0
*
*
*
SPD(μM) 0 50 100 200

346

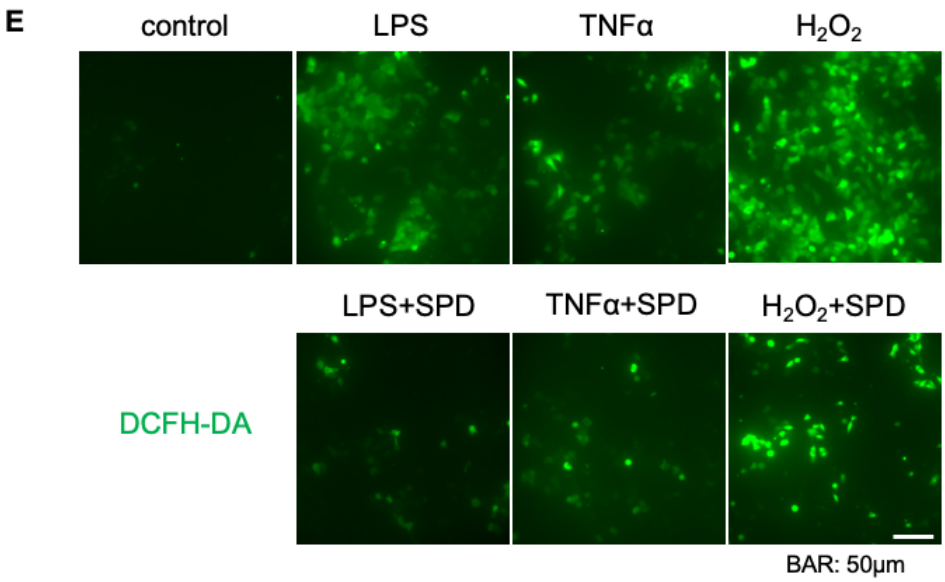
E
control
LPS
TNFα
H_2O_2
LPS+SPD
TNFα+SPD
H_2O_2+SPD
DCFH-DA
BAR: 50μm

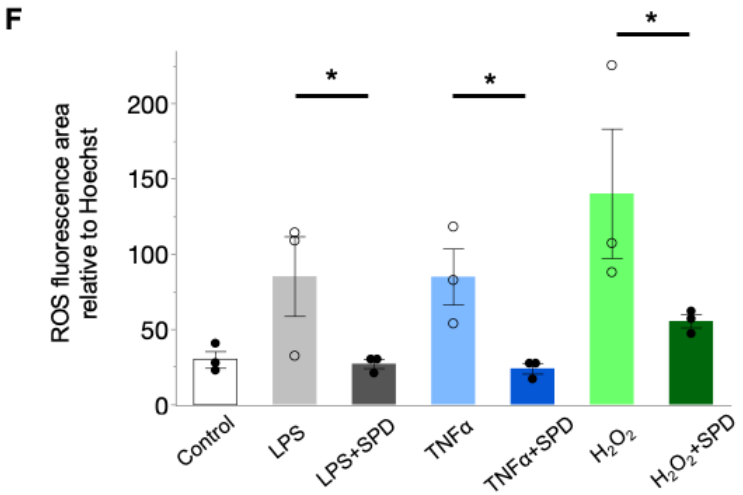
F
ROS fluorescence area relative to Hoechst
200
150
100
50
0
*
*
*
Control
LPS
LPS+SPD
TNFα
TNFα+SPD
H_2O_2
H_2O_2+SPD

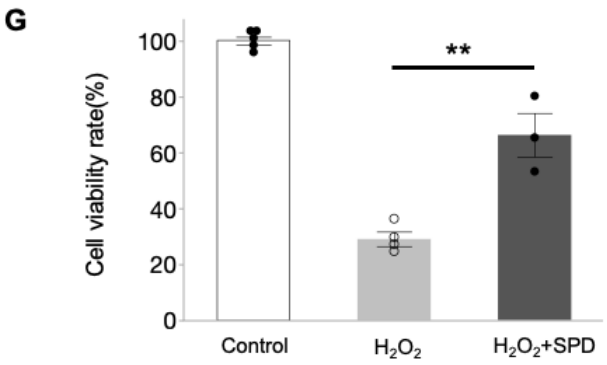
G
Cell viability rate(%)
100
80
60
40
20
0
**
Control
H_2O_2
H_2O_2+SPD

347

348

Fig. 2 Spermidine protects colonic epithelial cells from oxidative stress.

A Real-time PCR analysis of mRNA in HCT116 cells treated with 50 μM SPD for 12 h. Antioxidant gene expression was elevated (n = 3 in each group).

B Western blotting analysis of indicated proteins in HCT116 cells with and without 50 μM SPD treatment for 24 h. Antioxidant gene protein expression was enhanced. ß-actin is shown as the loading control.

C Western blotting analysis of nuclear proteins after treatment with SPD at the indicated concentration for 24 h.

D Nuclear NRF2 protein expression standardized by HDAC2 protein expression was increased after SPD treatment.

E Fluorescent images of intracellular ROS analyzed by DCFH-DA. The upper panels show the cells stimulated with LPS (500 ng/ml), TNFα (50 ng/ml), and H_2O_2 (250 μM) for 24 h. The lower panels show these cells treated with SPD (50 μM). Bar = 50 μm.

F Intracellular ROS was evaluated by the fluorescence area relative to Hoechst. Stimulation by LPS, TNFα, and H_2O_2 increased intracellular ROS, and treatment with SPD suppressed this increased ROS (n = 3 in each group).

G Cell viability was evaluated by the MTT assay. Cell death was induced by H_2O_2 (800 μM) and the cells were treated with SPD (50 μM) for 24 h (n = 4 in each group).

The results are expressed as the mean ± standard error. The unpaired t test or Turkey–Kramer's test was used for analysis. *$P < 0.05$ and **$P < 0.01$. Abbreviations: ARG2; arginase 2, GCLM; glutamate-cysteine ligase modifier subunit, HDAC2; histone deacetylase 2, HO-1; heme oxygenase-1, H_2O_2; hydrogen peroxide, LPS; lipopolysaccharide, MTT; 3-[4,5-dimethylthiazol-2-yl]-2,5-diphenyltetrazolium bromide, NRF2; nuclear factor erythroid 2-related factor2, NQO1; nicotinamide

quinone oxidoreductase 1, ROS; reactive oxygen species, SPD; spermidine, TNFα; tumor necrosis factor-α, TXNR; thioredoxin reductase 1.

Arg2 knockdown reduces polyamine production, decreases expression of NRF2-related antioxidant genes, and reduces antioxidant activity

The enzyme ARG2 converts arginine to polyamines, such as SPD, in the colonic epithelium. We investigated the effect of endogenous SPD in the *Arg2* knockdown cell line. Initially, we observed that polyamine production was increased in the HCT116 cell line upon exposure to various stimuli (LPS and TNFα). However, in the *Arg2* knockdown group, polyamine production was diminished compared with the TNFα group (Figure 3A, B).

Furthermore, we found that oxidative stress by H_2O_2 upregulated *HO-1* and *GCLM* mRNA transcription, but this effect was abolished by *Arg2* knockdown (Figure 3C and D). Similarly, HO-1 protein expression in response to H_2O_2 stimulation was limited by *Arg2* knockdown (Figure 3E).

Cell viability was compared in response to oxidative stress, and we observed a decrease in viability in the *Arg2* knockdown group compared with that of non-knockdown group. (Figure 3F). These results suggest that SPD production via the enzyme ARG2 plays a crucial role in activating the antioxidant effect in colonic epithelium.

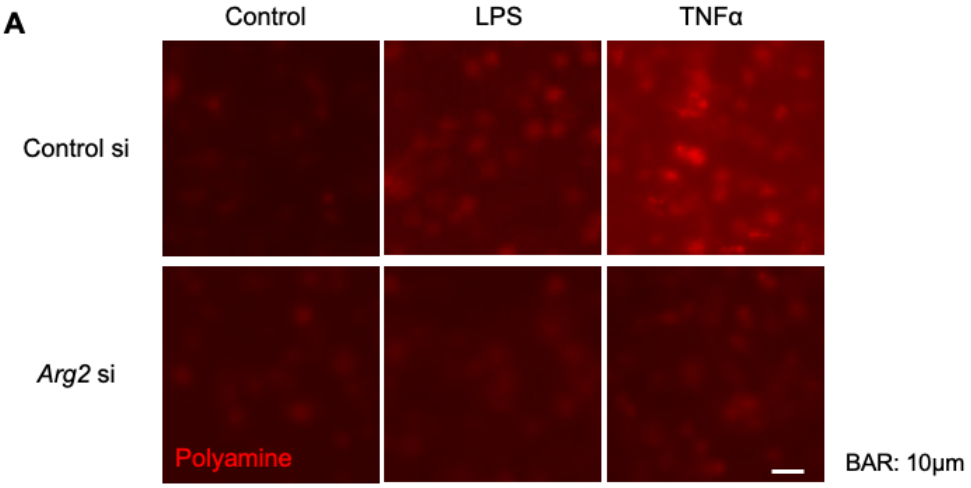
A
Control
LPS
TNFα
Control si
Arg2 si
Polyamine
BAR: 10μm

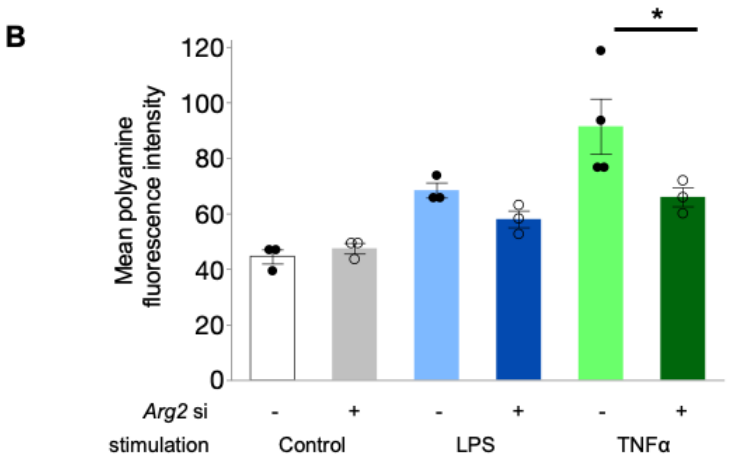
B
Mean polyamine fluorescence intensity
120
100
80
60
40
20
0
*
Arg2 si - + - + - +
stimulation Control LPS TNFα

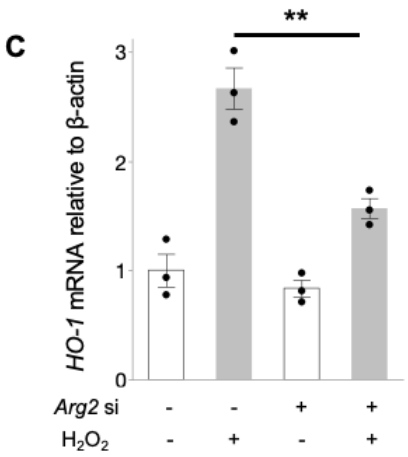
C
HO-1 mRNA relative to β-actin
3
2
1
0
**
Arg2 si - - + +
H2O2 - + - +

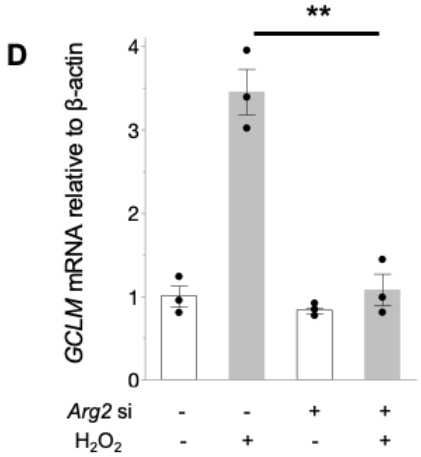
D
GCLM mRNA relative to β-actin
4
3
2
1
0
**
Arg2 si - - + +
H2O2 - + - +

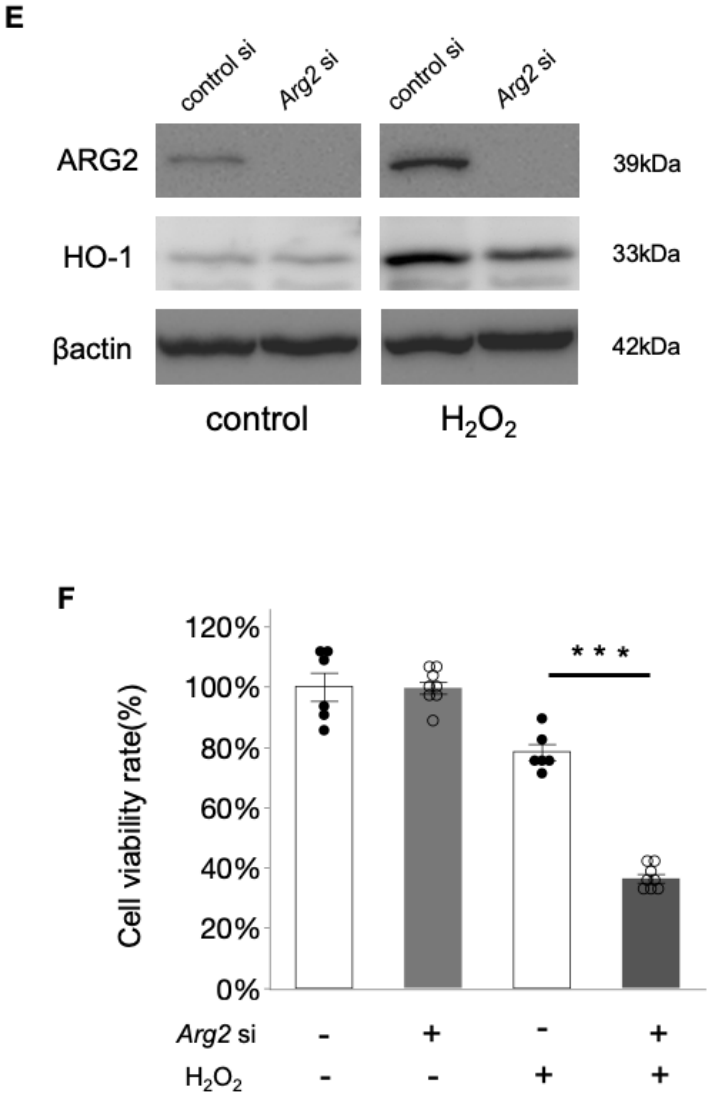

394

395 **Fig. 3 The antioxidant effect is attenuated in *Arg2* knockdown cells.**

396 **A** Polyamine staining in control (upper panel) and *Arg2* (lower panel) knockdown cells

397 is shown. The cells were stimulated with LPS (500 ng/ml) and TNFα (50 ng/ml) for 24

398 h. Bar = 10 μm.

399 **B** Intracellular polyamine accumulation was assessed by the mean fluorescence

400 intensity in control and *Arg2* knockdown cells. The polyamine accumulation level was

lower in the *Arg2* knockdown cells stimulated with TNFα compared with that of non-knockdown cells (n = 4 in the *Arg2* knockdown and TNFα stimulation group, n=3 in the other groups).

C *HO-1* mRNA expression was analyzed by real-time PCR. HO-1 mRNA expression levels were lower in *Arg2* knockdown cells stimulated with H_2O_2 (1000 μM) for 12 h compared with that of non-knockdown cells.

D Real-time PCR shows decreased *GCLM* mRNA expression in *Arg2* knockdown cells stimulated with H_2O_2 (1000 μM) for 12 h compared with that of non-knockdown cells.

E Western blot analysis shows that HO-1 protein levels were lower in *Arg2* knockdown cells than in controls in the presence of H_2O_2 (1000 μM) for 24 h.

F Cell viability was compared between control and *Arg2* knockdown cells in the absence or presence of H_2O_2 (700 μM) for 24 h. The cell viability rate was lower in *Arg2* knockdown cells than in controls in the presence of H_2O_2.

The results are expressed as the mean ± standard error. Turkey–Kramer's test was used for analysis. *P < 0.05, **P < 0.01 and ***P < 0.001. Abbreviations: ARG2; arginase 2, GCLM; glutamate-cysteine ligase modifier subunit, HO-1; heme oxygenase-1, H_2O_2; hydrogen peroxide, LPS; lipopolysaccharide, TNFα; tumor necrosis factor-α.

DSS-induced colitis in *Arg*2 KO mice is exacerbated by intestinal inflammation compared with WT mice

To evaluate the role of SPD *in vivo*, we compared WT and *Arg2* KO mice using the DSS colitis model. First, we examined SPD accumulation in DSS colitis using fluorescent antibody immunostaining. WT mice displayed a higher accumulation of SPD in DSS colitis than that in *Arg2* KO mice (Figure 4A and B).

Subsequently, we compared the severity of DSS colitis in WT and *Arg2* KO mice. We analyzed the rate of change in body weight over time between the two groups. Although there was no significant difference in the change in body weight between the groups, the KO group showed a tendency towards a lower body weight on day 5 (Figure 4C). The stool consistency score was significantly higher and the colon length was significantly shorter in the *Arg2* KO group than in the WT group (Figure 4D and E).

We further assessed the severity of intestinal pathology in both groups. Representative pathological specimens of HE-stained images from the WT and *Arg2* KO groups are shown in Figure 4F. The total pathological score was evaluated by adding the inflammation, ulceration, hyperplasia, and disease area scores. The *Arg2* KO group showed significantly more severity than the WT group (Figure 4G). In addition, proteins were extracted and assessed for proteins of NRF2-related genes. The WT group, but not the KO group, showed increased HO-1 and GCLM protein expression in DSS colitis (Figure 4H). These findings suggest that ARG2 has an inhibitory effect on DSS colitis through the production of SPD.

Organoids extracted and cultured from *Arg2* KO mice show reduced resistance to oxidative stress compared with those from WT mice

Organoids were generated from the crypts of the small intestine (Figure 4I, J) and the colon (Figure 4K) in WT and *Arg2* KO mice via *in vitro* culture. They were subsequently subjected to oxidative stress via H_2O_2 stimulation to compare their respective viability rates. The organoids derived from the small intestine and the colon of *Arg2* KO mice both showed significantly lower survival rates than those of the WT-derived organoids (Figure 4J, K). These findings suggest that the heightened

449 susceptibility of the intestinal epithelium to oxidative stress contributes to the worsening
450 of colitis.

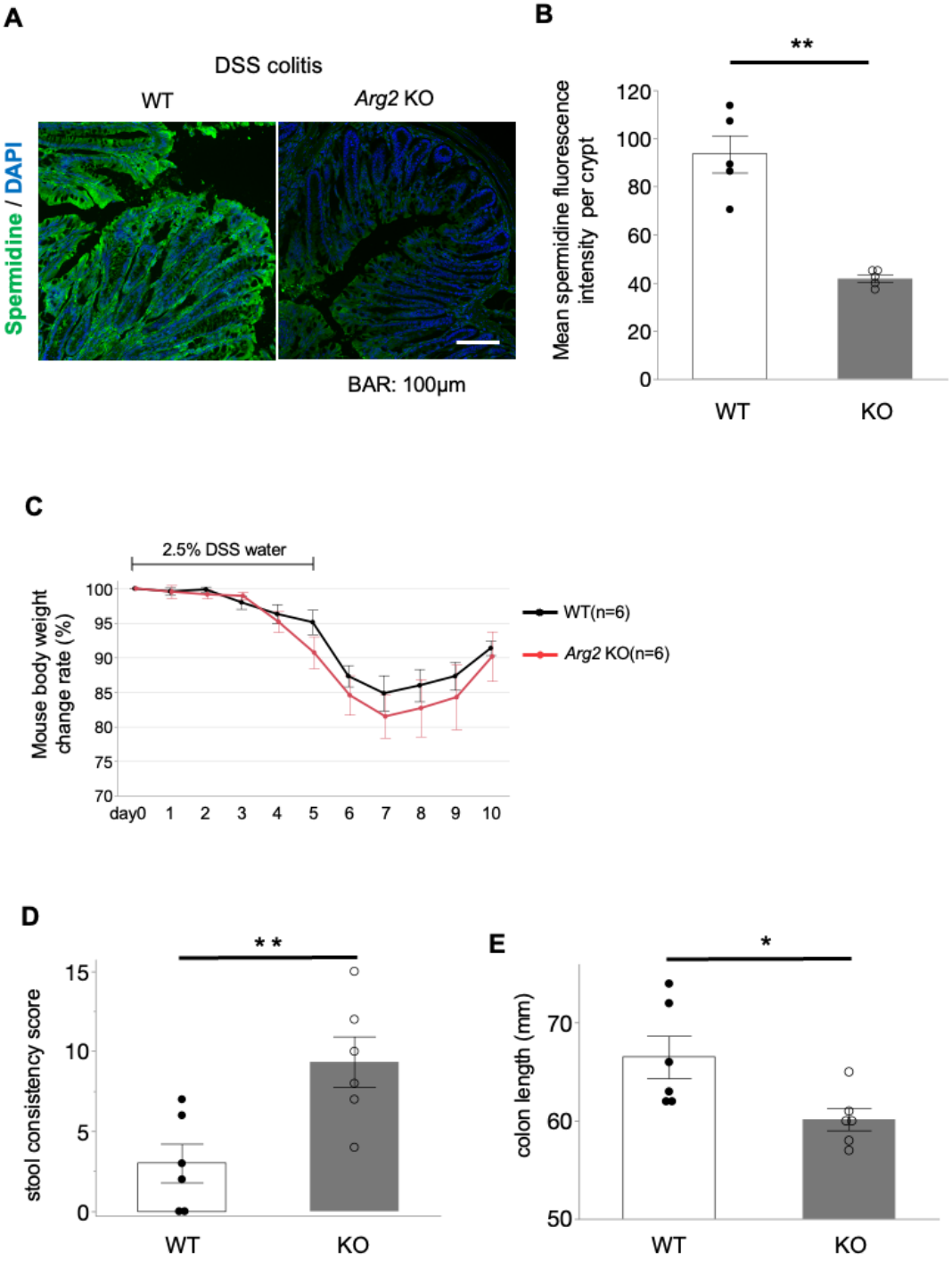
A
DSS colitis
WT
Arg2 KO
Spermidine / DAPI
BAR: 100μm
B
**
Mean spermidine fluorescence intensity per crypt
120
100
80
60
40
20
0
WT
KO
C
2.5% DSS water
Mouse body weight change rate (%)
100
95
90
85
80
75
70
day0 1 2 3 4 5 6 7 8 9 10
WT(n=6)
Arg2 KO(n=6)
D
**
stool consistency score
15
10
5
0
WT
KO
E
*
colon length (mm)
70
60
50
WT
KO

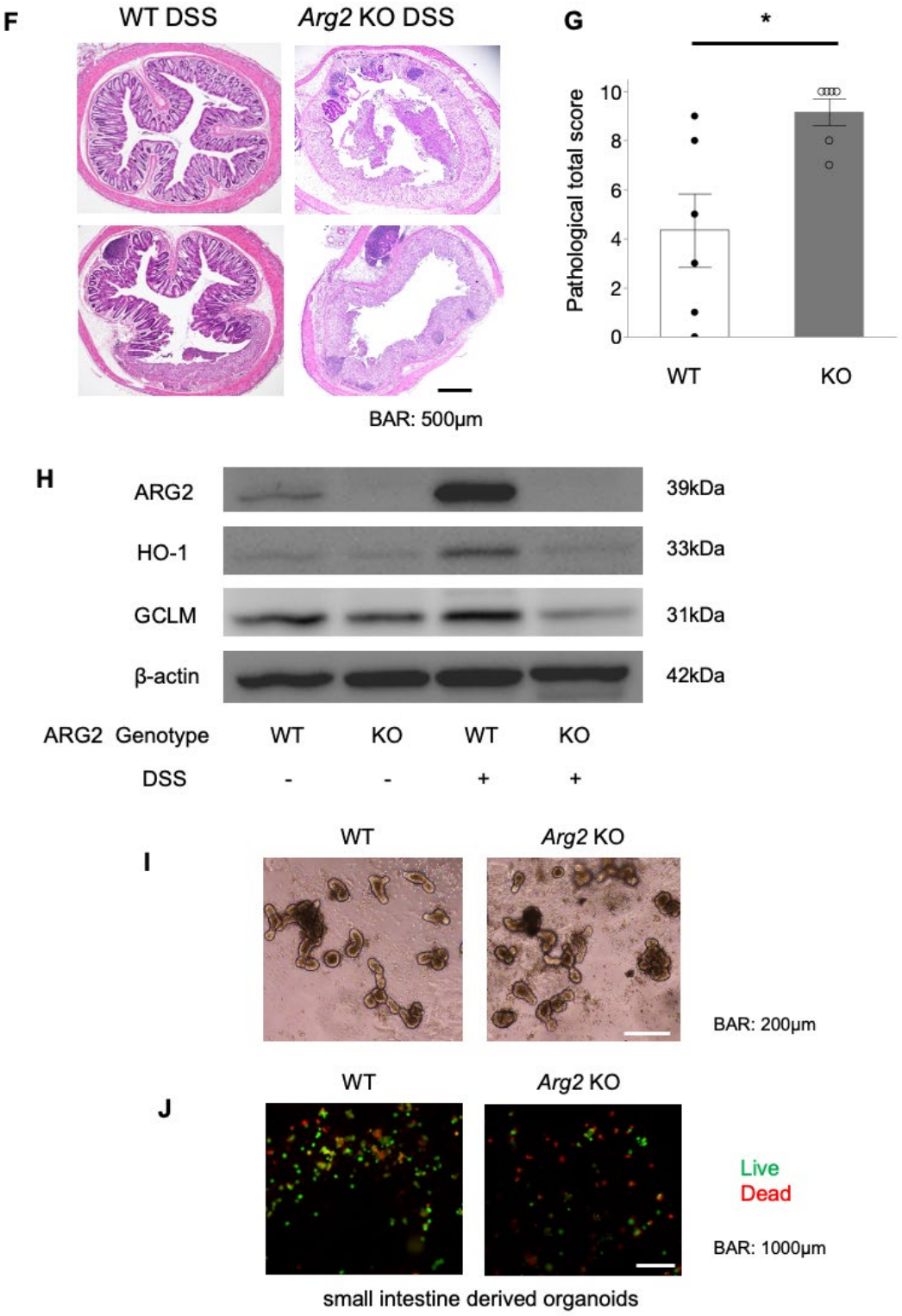
F
WT DSS
Arg2 KO DSS
BAR: 500μm
G
*
Pathological total score
10
8
6
4
2
0
WT
KO
H
ARG2
HO-1
GCLM
β-actin
39kDa
33kDa
31kDa
42kDa
ARG2 Genotype WT KO WT KO
DSS - - + +
I
WT
Arg2 KO
BAR: 200μm
J
WT
Arg2 KO
Live
Dead
BAR: 1000μm
small intestine derived organoids

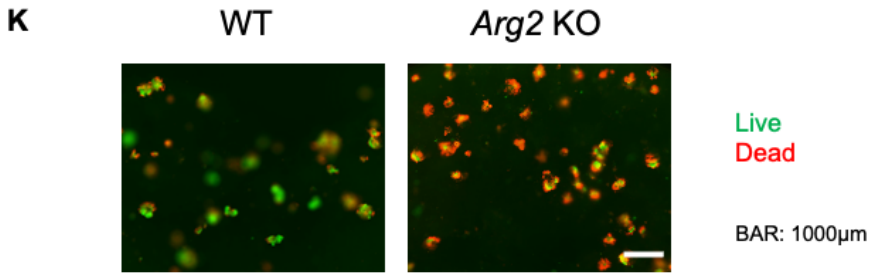

Fig. 4 DSS colitis is exacerbated in *Arg*2 KO mice.

A Representative immunohistochemical staining with anti-SPD antibodies was performed in the distal colon in WT and *Arg2* KO mice with DSS colitis. Bar = 100 μm.

B Fluorescence intensity of SPD in each crypt is shown. In DSS colitis, the colon of *Arg2* KO mice accumulated less SPD than that in WT mice (n = 5 in each group).

C Changes in body weight in both groups are shown (n = 6 in each group).

D Total 10-day stool consistency scores were compared between the WT and Arg2 KO groups (n = 6 in each group). *Arg2* KO mice showed a worse stool consistency score than WT mice.

E The length of the colon at day 10 was compared between WT and *Arg2* KO mice (n = 6 in each group). The colon length was shorter in the *Arg2* KO group than in the WT group.

F Representative images (HE staining) of the distal colon show severe colitis in *Arg2* KO mice. Bar = 500 μm.

G The pathological score shows that colitis was severe in *Arg2* KO mice (n = 6 in each group).

H Expression of protein in the colon was evaluated by western blotting. In DSS colitis, HO-1 and GCLM protein expression was lower in *Arg2* KO mice than in WT mice.

I Extracted from WT and Arg2 KO mice and cultured organoids derived from small

intestine. Organoids are shown at the time of sufficient maturation. There were no obvious differences in organoid morphology between WT and Arg2 KO derived organoids. Bar = 200 μm.

J Small intestine-derived organoid viability was analyzed after treatment with H_2O_2 (500 μM) for 24 h. The live organoids are stained green and the dead organoids are stained red. The live: dead ratio was as follows: WT, 105:21 vs *Arg2* KO, 67:68 ($P < 0.001$). Bar = 1000 μm.

K Colon-derived organoid viability was also analyzed after treatment with H_2O_2 (500 μM) for 24 h. The live organoids are stained green and the dead organoids are stained red. The live: dead ratio was as follows: WT, 26:14 vs *Arg2* KO, 10:99 ($P < 0.001$). Bar = 1000 μm.

The results are expressed as the mean ± standard error. The unpaired t test and chi-square test were used for analysis. *$P < 0.05$ and **$P < 0.01$. Abbreviations: ARG2; arginase 2, DAPI; 4,6-diamino-2-phenylindole, DSS; dextran sulfate sodium, GCLM; glutamate-cysteine ligase modifier subunit, HO-1; heme oxygenase-1, WT; wild type.

Oral supplementation of SPD ameliorates DSS colitis in both WT and *Arg2* KO mice

Next, we examined whether the exacerbation of colitis induced by *Arg2* deficiency could be ameliorated by SPD administration. In both WT and *Arg2* KO mice groups, mice receiving SPD supplementation showed milder DSS induced colitis with reduced body weight loss (Figure 5A, B), lower stool consistency scores (Figure 5C), and significantly longer colon length (Figure 5D) compared to mice not receiving supplementation. Furthermore, representative pathological specimens of HE-stained images are shown in Figure 5E. In both WT and *Arg2* KO mice, those receiving SPD supplementation had

497 significantly lower total histological scores compared to mice not receiving
498 supplementation (Figure 5F). Despite DSS induced colitis being more severe in Arg2 KO
499 mice compared to WT mice, supplementation with SPD result in comparable severity of
500 colitis in both Arg2 and WT mice as demonstrating in stool consistency scores (Fig 5C),
501 colon length (Fig 5D), and pathological scores (Fig 5E). These findings suggest that the
502 severe colitis in Arg2 KO mice may be attributed to reduced levels of SPD.

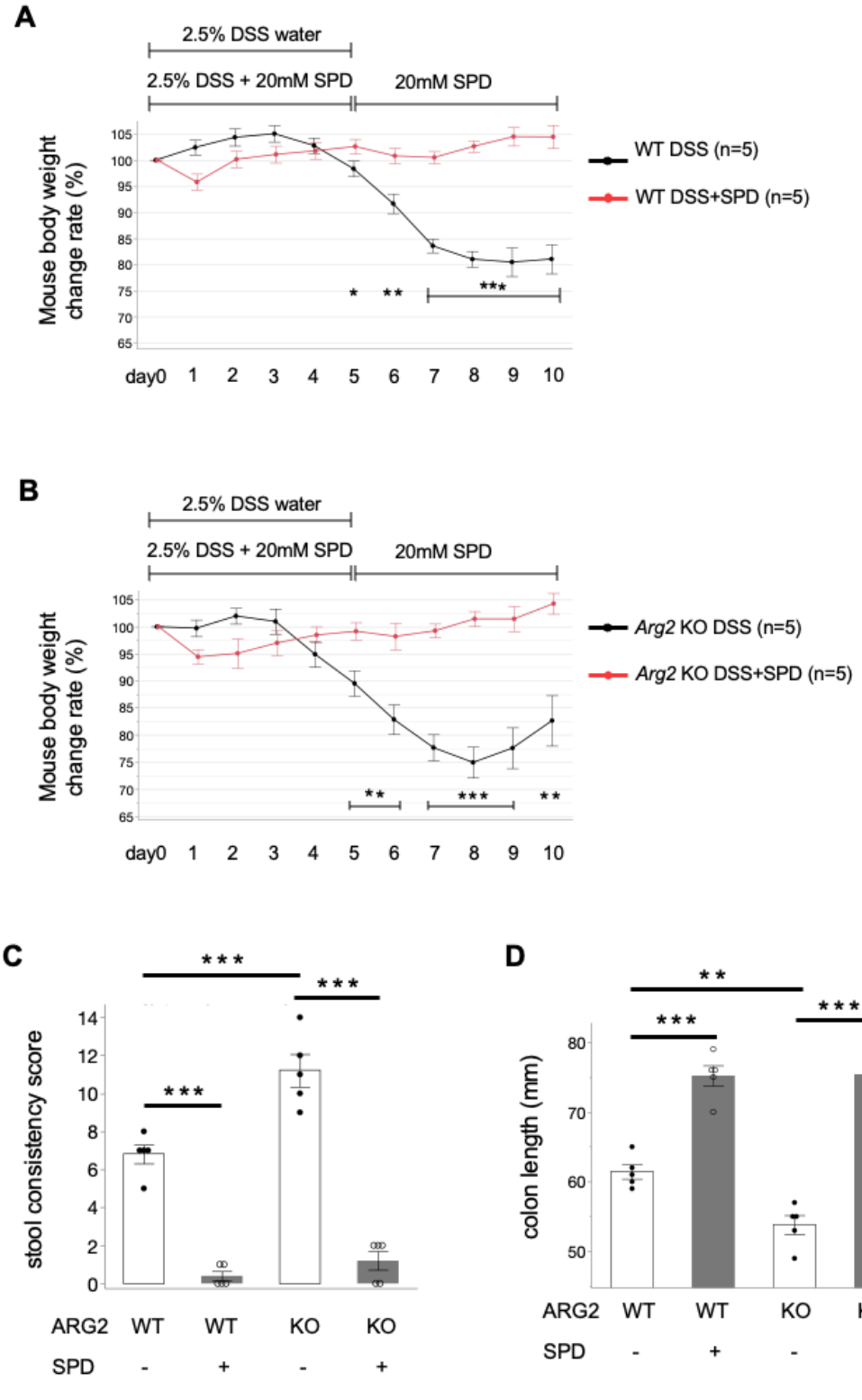
A
2.5% DSS water
2.5% DSS + 20mM SPD
20mM SPD
Mouse body weight change rate (%)
WT DSS (n=5)
WT DSS+SPD (n=5)
day0 1 2 3 4 5 6 7 8 9 10
B
2.5% DSS water
2.5% DSS + 20mM SPD
20mM SPD
Mouse body weight change rate (%)
Arg2 KO DSS (n=5)
Arg2 KO DSS+SPD (n=5)
day0 1 2 3 4 5 6 7 8 9 10
C
stool consistency score
ARG2 WT WT KO KO
SPD - + - +
D
colon length (mm)
ARG2 WT WT KO KO
SPD - + - +

503

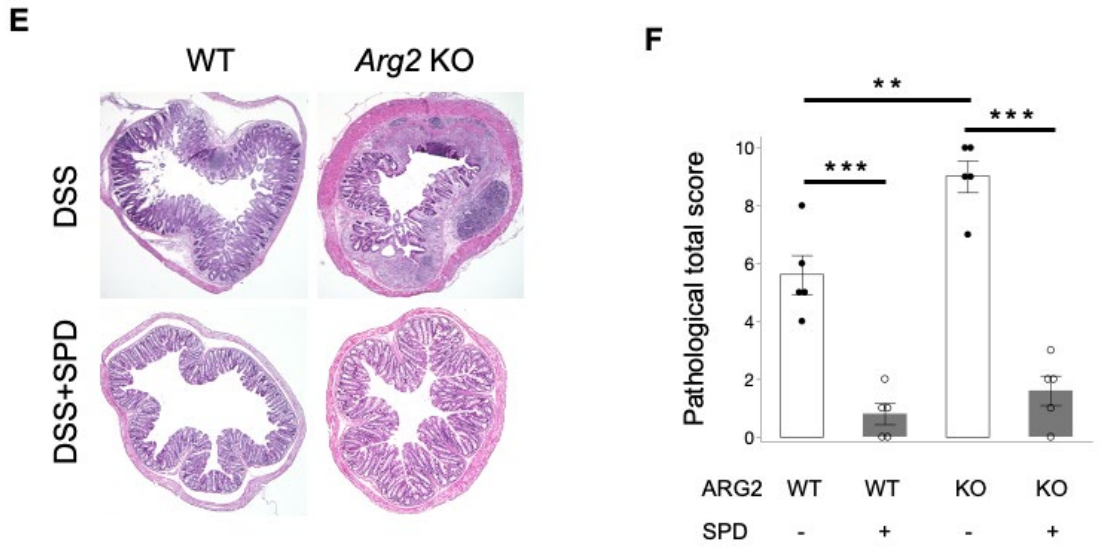

504

505 **Fig. 5 SPD supplementation ameliorates DSS colitis.**

506 **A** Changes in body weight in DSS with SPD group and DSS alone group in WT mice (n
507 = 5 in each group). The body weight of DSS+SPD groups was significantly higher than
508 that of DSS alone groups from day 5 to day 10.

509 **B** Changes in body weight in DSS with SPD group and DSS alone group in *Arg2* KO
510 mice (n = 5 in each group). The body weight of DSS+SPD groups was significantly
511 higher from day 5 to day 10.

512 **C** Total stool consistency scores are shown over the 10-day period for DSS+SPD and
513 DSS alone groups in both WT and *Arg2* KO mice (n = 5 in each group). The DSS+SPD
514 groups showed significantly lower scores compared to the DSS alone groups in each
515 genotype.

516 **D** The length of the colon at day 10 was compared between DSS+SPD and DSS alone
517 mice in WT and *Arg2* KO mice (n = 5 in each group). The colon length was longer in
518 the DSS+SPD group than DSS alone group in each genotype.

519 **E** Representative images (HE staining) of the distal colon show less severe colitis in the

DSS+SPD mice.

F The total pathological score shows that colitis was less severe in DSS+SPD mice compared to DSS alone mice in each genotype. (n = 5 in each group).

The results are expressed as the mean ± standard error. The unpaired t test and Turkey–Kramer's test were used for analysis. *P < 0.05, **P < 0.01 and ***P < 0.001. Abbreviations: ARG2; arginase 2, DSS; dextran sulfate sodium, KO; knockout, SPD; spermidine, WT; wild type.

Human UC intestinal epithelium shows higher ARG2 protein expression and SPD accumulation in the active phase than in the remission phase

To investigate the involvement of ARG2 and SPD in UC, fluorescent antibody immunostaining was conducted in human UC intestinal epithelium obtained from biopsy tissue during the active and remission phases (Figure 6A, D). In addition, we investigated *Arg2* mRNA levels using quantitative real-time PCR (Figure 6C). We found that ARG2 (Figure 6B, C) and SPD (Figure 6E) were significantly upregulated in the active phase compared with the remission phase in intestinal epithelium. Moreover, we also compared ARG2 expression and SPD accumulation of the rectal mucosa between healthy controls without gastrointestinal disease and UC patients in remission by fluorescent immunochemical staining (Fig 6F, H). There was no significant difference in ARG2 and SPD between healthy control and UC patients in remission phase (Fig 6G, I). These findings suggest that ARG2 and SPD are implicated in the pathogenesis of human UC in addition to the DSS colitis model.

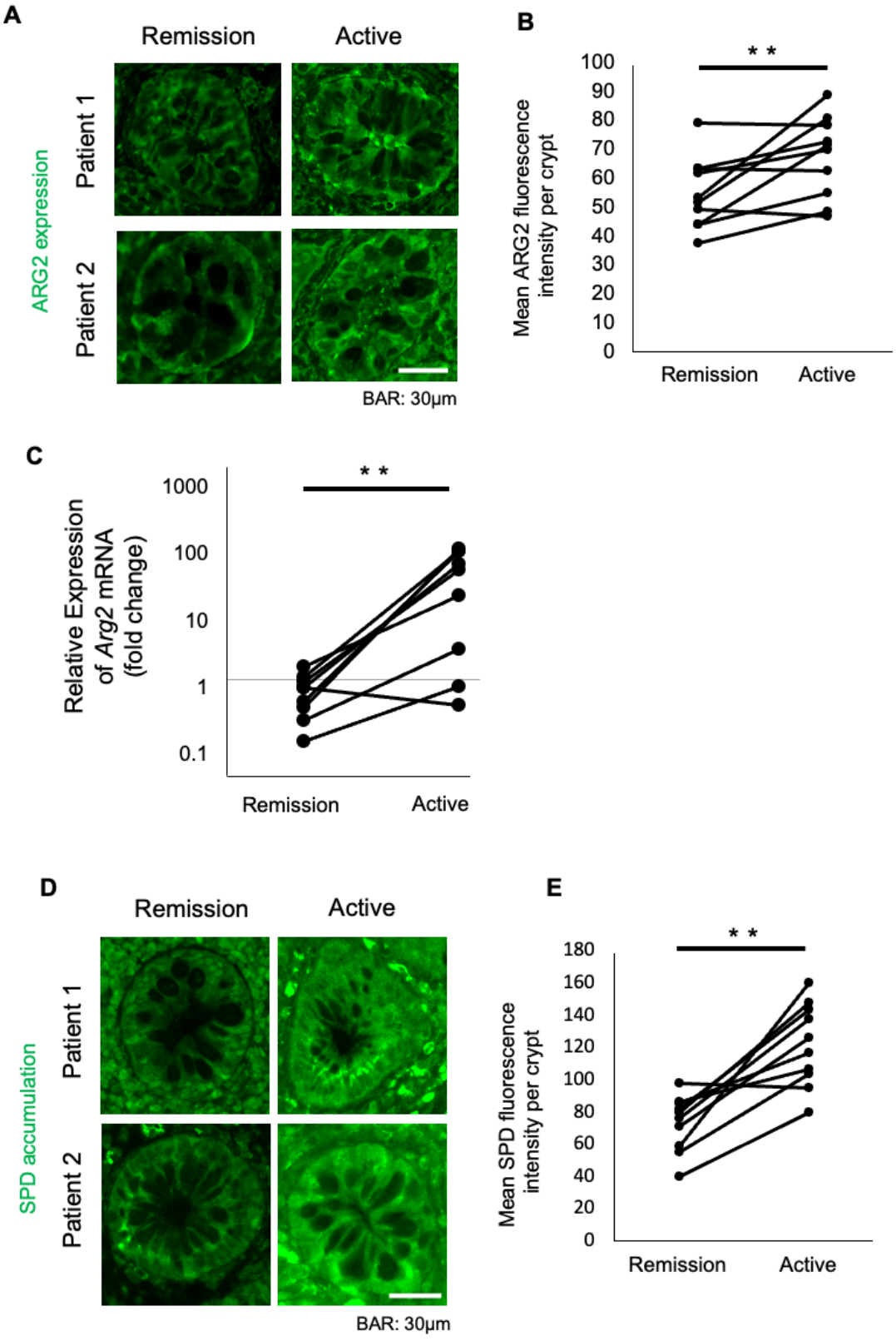
A
Remission
Active
ARG2 expression
Patient 1
Patient 2
BAR: 30μm
B
Mean ARG2 fluorescence intensity per crypt
100
90
80
70
60
50
40
30
20
10
0
* *
Remission
Active
C
Relative Expression of Arg2 mRNA (fold change)
1000
100
10
1
0.1
* *
Remission
Active
D
Remission
Active
SPD accumulation
Patient 1
Patient 2
BAR: 30μm
E
Mean SPD fluorescence intensity per crypt
180
160
140
120
100
80
60
40
20
0
* *
Remission
Active

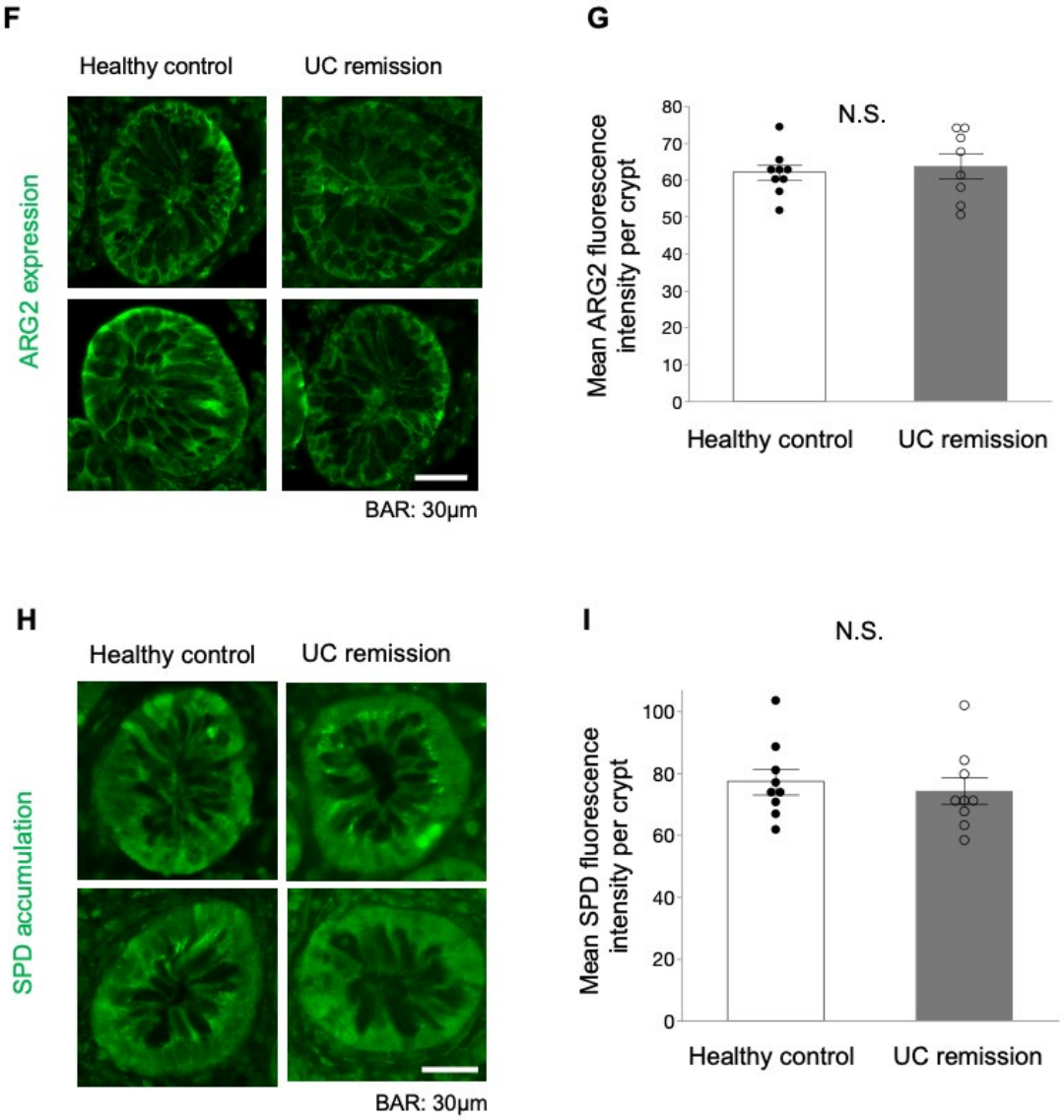

Fig. 6 Intestinal epithelium in patients with active UC shows increased ARG2 protein expression and accumulation of SPD.

A Representative immunohistochemical staining of ARG2 in patients with UC. The mucosa from the same patients was obtained in the active and remission phases. Bar = 30 μm.

B ARG2 fluorescence intensity in the crypts was significantly higher during the active phase than in the remission phase (n = 10).

C Real-time PCR analysis of mRNA of *Arg2* obtained from rectal mucosa in patients

552 with UC. mRNA level was significantly higher in active phase than in the remission
553 phase (n=9).
554 **D** Representative images of SPD in patients with UC. The mucosa from the same
555 patients was obtained in the active and remission phases. Bar = 30 μm.
556 **E** SPD accumulation was significantly higher in the active phase than in the remission
557 phase (n = 10).
558 **F** Immunohistochemical was performed on biopsy tissue from the rectal mucosa of
559 healthy control patients without gastrointestinal disease. Representative images of
560 ARG2 in patients with healthy control and UC in remission phase.
561 **G** There was no significant difference in ARG2 fluorescence intensity between healthy
562 control (n=9) and UC patients in remission phase (n=8).
563 **H** Representative images of SPD in patients with healthy control and UC in remission
564 phase.
565 **I** There was no significant difference in SPD accumulation between healthy control and
566 UC patients in remission phase (n=9).
567 The paired-samples t test and the unpaired t test was used for analysis. **P < 0.01.
568 Abbreviations: ARG2; arginase 2, N.S.; not significant, SPD; spermidine.
569
570
571
572
573
574
575

576 **Discussion**

577 In this study, we found that SPD, which is synthesized from L-Arg by the enzyme
578 ARG2, plays a critical role in the suppression of DSS colitis. Numerous reports have
579 suggested the protective effects of L-Arg supplementation on DSS enteritis models. [17]
580 [26] [27] [28] Furthermore, active human UC shows decreased L-Arg levels in tissue
581 and increased *Arg2* mRNA levels [29], indicating an association between arginine
582 metabolism and IBD. Nevertheless, the underlying mechanism of this relationship
583 remains obscure. In the current study, we showed that endogenous SPD exerted anti-
584 inflammatory effects through the suppression of oxidative stress.
585 Elevated levels of SPD have been reported in the intestinal mucosa of patients with
586 UC compared with healthy individuals [11] [12]. The physiological role of SPD is
587 essential for maintaining normal cellular growth and function, and its intracellular
588 concentrations are intricately regulated [30]. SPD prolongs the life span and provides
589 protection to various organs. SPD also promotes anti-inflammatory macrophages and
590 inhibits colitis [31]. SPD was reported to inhibit liver fibrosis [32], prevent renal fibrosis
591 [33], show cardioprotective effects in a myocardial infarction model [34], and attenuate
592 brain aging [35]. During inflammation, SPD plays a role as a metabolic signal,
593 increasing its production in response to cell death and acting as a “goodbye” signal, and
594 promotes wound healing [36]. In the present study, we also observed elevated SPD
595 levels in the rectal mucosa in mice with DSS colitis and patients with UC. In *Arg2*-
596 deficient mice, decreased SPD levels were associated with exacerbated colitis,

indicating a protective role of SPD on the intestinal tract.

In this study, the increase in ARG2 and SPD in the rectal mucosa of active UC patients may be just a result of inflammation or a compensatory response to suppress inflammation, which remains open to debate. We showed the exacerbation of inflammation due to decreased SPD accumulation in ARG2-deficient mice, as well as the suppression of inflammation with SPD administration. Several other reports exist on the improvement of experimental colitis with SPD supplementation in SMOX-deficient mice [13], as well as on the control macrophage subtypes [31] and supplementation of bacterial-derived SPD in the gut [14]. While there are no clinical trials supplementing SPD in UC patients, there are reports suggesting reduced polyamine levels contribute to the exacerbation and chronicity of colitis [11]. These studies suggest that ARG2 and SPD contributes homeostatic mechanism during colitis.

The mechanism underlying the organ-protective effect of SPD is attributed to its ability to inhibit ROS as a free radical scavenger[37] and to promote the expression of antioxidant stress genes by activating NRF2. NRF2 is a stress-responsive transcription factor that helps maintain cellular homeostasis [38]. Activation of NRF2 is anticipated to contribute to anti-inflammatory therapy in the treatment of IBD[39]. In our study, SPD promoted the expression of genes, such as *HO-1*, *GCLM*, *TXNR*, and *NQO1*, through nuclear translocation of NRF2. HO-1 plays a role in protecting against oxidative damage, regulating apoptosis, and modulating inflammation [40]. GCLM catalyzes glutathione biosynthesis [41] [42], and NQO1 prevents the formation of ROS by detoxifying quinones.[41] This study showed that SPD enhanced the expression of

antioxidants, reduced cellular production of ROS, and protected cells from ROS-induced cell death. In the absence of ARG2, SPD levels were decreased, leading to increased ROS levels and heightened cell death in response to oxidative stress. The antioxidant activity of SPD highlights its potential effectiveness in the treatment of UC.

While we focus on colonic epithelial cells since SPD was accumulated in mucosa during colitis, ARG2 plays a significant role on immune cells. ARG2 has been reported as mediator of IL-10 in inflammatory macrophage [43], and it controls T cell survival capacity [44]. These findings suggest that ARG2 deficiency may result in an inflammatory shift in immune cells.

Supplementation with L-arginine or SPD has an inhibitory effect on DSS colitis in mice. L-arginine is metabolized by arginase, leading to the production of SPD and nitric oxide through two pathways. However, nitric oxide production is elevated in patients with UC [45] [46], and nitric oxide can contribute to neutrophil infiltration and tissue damage [47]. Furthermore, while oral or external supplementation of SPD has been shown to have efficacy to ameliorate colitis [14], our study suggested the importance of endogenous SPD production mediated by ARG2. Our results obtained from organoids and cultured cells also indicated the contribution of SPD in inhibiting intestinal epithelial cell death. DSS colitis is exacerbated in mice with spermine oxidase KO, which is an alternative endogenous pathway for SPD production independent of ARG2 [13]. This finding suggests the importance of endogenous SPD and its regulatory mechanisms in the development of colitis.

In summary, this study shows that endogenous production of polyamines, especially

641 SPD, through the action of arginase, plays a crucial role in protecting the intestinal
642 mucosa by exerting antioxidant effects on the intestinal epithelium. Targeting this
643 mechanism could be a promising therapeutic approach for IBD, including UC.
644
645 **Acknowledgements**
646 We appreciate the technical support from the Research Support Center, Graduate School
647 of Medical Sciences, Kyushu University. We also thank Mr. M. Munakata and Mrs. M
648 Tanaka at the Department of Medicine and Clinical Science, Graduate School of Medical
649 Sciences, Kyushu University for assistance with histology. We thank Ellen Knapp, PhD,
650 from Edanz Group (https://jp.edanz.com/ac) for editing a draft of this manuscript. We
651 acknowledge BioRender.com to create graphic abstract.
652
653 **Authors' contributions**
654 NI, and TT conceived the idea of the study. NI, AY, SK, T. Nitahata, YU, SA, and TT
655 were involved in providing guidance on the animal experiments and data analysis. JU,
656 KK, SF, YF, YM, T. Nagasue, TM, YT, and TT collected the clinical samples and
657 contributed to interpretation of the data. TK, YO and TT contributed to drafting of the
658 manuscript and critical revision. All authors revised the manuscript, approved the
659 manuscript to be published, and agree to be accountable for all aspects of the work.
660
661 **Funding**
662 This work was supported by JSPS KAKENHI [Grant No. JP21K06783] and a Grant-in-
663 Aid for Scientific Research C.
664

Ethics declarations

Conflict of Interest Statement

The authors declare that they have no conflict of interest.

References

1. Kobayashi T, Siegmund B, Le Berre C, et al. Ulcerative colitis. Nat Rev Dis Primers. 2020;6:74.
2. Ng SC, Shi HY, Hamidi N, et al. Worldwide incidence and prevalence of inflammatory bowel disease in the 21st century: a systematic review of population-based studies. Lancet. 2017;390:2769-78.
3. Nakase H, Sato N, Mizuno N, et al. The influence of cytokines on the complex pathology of ulcerative colitis. Autoimmun Rev. 2022;21:103017.
4. Beaugerie L, Rahier JF, Kirchgesner J. Predicting, Preventing, and Managing Treatment-Related Complications in Patients With Inflammatory Bowel Diseases. Clin Gastroenterol Hepatol. 2020;18:1324-35 e2.
5. Ihara Y, Torisu T, Miyawaki K, et al. Ustekinumab Improves Active Crohn's Disease by Suppressing the T Helper 17 Pathway. Digestion. 2021;102:946-55.
6. Imazu N, Torisu T, Ihara Y, et al. Ustekinumab Decreases Circulating Th17 Cells in Ulcerative Colitis. Intern Med. 2023.
7. Madeo F, Hofer SJ, Pendl T, et al. Nutritional Aspects of Spermidine. Annu Rev Nutr. 2020;40:135-59.
8. Zou D, Zhao Z, Li L, et al. A comprehensive review of spermidine: Safety, health effects, absorption and metabolism, food materials evaluation, physical and chemical processing, and bioprocessing. Compr Rev Food Sci Food Saf. 2022;21:2820-42.
9. Eisenberg T, Knauer H, Schauer A, et al. Induction of autophagy by spermidine promotes longevity. Nat Cell Biol. 2009;11:1305-14.
10. Timmons J, Chang ET, Wang JY, et al. Polyamines and Gut Mucosal Homeostasis. J Gastrointest Dig Syst. 2012;2.
11. Weiss TS, Herfarth H, Obermeier F, et al. Intracellular polyamine levels of intestinal epithelial cells in inflammatory bowel disease. Inflamm Bowel Dis. 2004;10:529-35.
12. Obayashi M, Matsui-Yuasa I, Matsumoto T, et al. Polyamine metabolism in colonic mucosa from patients with ulcerative colitis. Am J Gastroenterol. 1992;87:736-40.
13. Gobert AP, Latour YL, Asim M, et al. Protective Role of Spermidine in Colitis and Colon Carcinogenesis. Gastroenterology. 2022;162:813-27 e8.
14. Nakamura A, Kurihara S, Takahashi D, et al. Symbiotic polyamine metabolism regulates epithelial proliferation and macrophage differentiation in the colon. Nat Commun. 2021;12:2105.
15. Yu H, Yoo PK, Aguirre CC, et al. Widespread expression of arginase I in mouse tissues. Biochemical and physiological implications. J Histochem Cytochem. 2003;51:1151-60.
16. Choi S, Park C, Ahn M, et al. Immunohistochemical study of arginase 1 and 2 in various tissues of rats. Acta Histochem. 2012;114:487-94.
17. Coburn LA, Gong X, Singh K, et al. L-arginine supplementation improves responses to injury and inflammation in dextran sulfate sodium colitis. PLoS One. 2012;7:e33546.
18. Zwintscher NP, Shah PM, Salgar SK, et al. Hepatocyte growth factor, hepatocyte growth factor activator and arginine in a rat fulminant colitis model. Ann Med Surg (Lond). 2016;7:97-103.
19. Kudo T, Matsumoto T, Nakamichi I, et al. Recombinant human granulocyte colony-stimulating factor reduces colonic epithelial cell apoptosis and ameliorates murine dextran sulfate sodium-induced colitis. Scand J Gastroenterol. 2008;43:689-97.
20. Hara M, Torisu K, Tomita K, et al. Arginase 2 is a mediator of ischemia-reperfusion injury in the

kidney through regulation of nitrosative stress. Kidney Int. 2020;98:673-85.
21. Sakuma S, Abe M, Kohda T, et al. Hydrogen peroxide generated by xanthine/xanthine oxidase system represses the proliferation of colorectal cancer cell line Caco-2. J Clin Biochem Nutr. 2015;56:15-9.
22. Kawano S, Torisu T, Esaki M, et al. Autophagy promotes degradation of internalized collagen and regulates distribution of focal adhesions to suppress cell adhesion. Biol Open. 2017;6:1644-53.
23. Li B, Alli R, Vogel P, et al. IL-10 modulates DSS-induced colitis through a macrophage-ROS-NO axis. Mucosal Immunol. 2014;7:869-78.
24. Torisu T, Torisu K, Lee IH, et al. Autophagy regulates endothelial cell processing, maturation and secretion of von Willebrand factor. Nat Med. 2013;19:1281-7.
25. Bajic D, Niemann A, Hillmer AK, et al. Gut Microbiota-Derived Propionate Regulates the Expression of Reg3 Mucosal Lectins and Ameliorates Experimental Colitis in Mice. J Crohns Colitis. 2020;14:1462-72.
26. Ren W, Yin J, Wu M, et al. Serum amino acids profile and the beneficial effects of L-arginine or L-glutamine supplementation in dextran sulfate sodium colitis. PLoS One. 2014;9:e88335.
27. Andrade ME, Santos RD, Soares AD, et al. Pretreatment and Treatment With L-Arginine Attenuate Weight Loss and Bacterial Translocation in Dextran Sulfate Sodium Colitis. JPEN J Parenter Enteral Nutr. 2016;40:1131-9.
28. Singh K, Gobert AP, Coburn LA, et al. Dietary Arginine Regulates Severity of Experimental Colitis and Affects the Colonic Microbiome. Front Cell Infect Microbiol. 2019;9:66.
29. Coburn LA, Horst SN, Allaman MM, et al. L-Arginine Availability and Metabolism Is Altered in Ulcerative Colitis. Inflamm Bowel Dis. 2016;22:1847-58.
30. Wallace HM, Fraser AV, Hughes A. A perspective of polyamine metabolism. Biochem J. 2003;376:1-14.
31. Niechcial A, Schwarzfischer M, Wawrzyniak M, et al. Spermidine ameliorates colitis via induction of anti-inflammatory macrophages and prevention of intestinal dysbiosis. J Crohns Colitis. 2023.
32. Liu P, de la Vega MR, Dodson M, et al. Spermidine Confers Liver Protection by Enhancing NRF2 Signaling Through a MAP1S-Mediated Noncanonical Mechanism. Hepatology. 2019;70:372-88.
33. Aihara S, Torisu K, Uchida Y, et al. Spermidine from arginine metabolism activates Nrf2 and inhibits kidney fibrosis. Commun Biol. 2023;6:676.
34. Yan J, Yan JY, Wang YX, et al. Spermidine-enhanced autophagic flux improves cardiac dysfunction following myocardial infarction by targeting the AMPK/mTOR signalling pathway. Br J Pharmacol. 2019;176:3126-42.
35. Xu TT, Li H, Dai Z, et al. Spermidine and spermine delay brain aging by inducing autophagy in SAMP8 mice. Aging (Albany NY). 2020;12:6401-14.
36. Medina CB, Mehrotra P, Arandjelovic S, et al. Metabolites released from apoptotic cells act as tissue messengers. Nature. 2020;580:130-5.
37. Murray Stewart T, Dunston TT, Woster PM, et al. Polyamine catabolism and oxidative damage. J Biol Chem. 2018;293:18736-45.
38. Niture SK, Khatri R, Jaiswal AK. Regulation of Nrf2-an update. Free Radic Biol Med. 2014;66:36-44.
39. Piotrowska M, Swierczynski M, Fichna J, et al. The Nrf2 in the pathophysiology of the intestine: Molecular mechanisms and therapeutic implications for inflammatory bowel diseases. Pharmacol Res. 2021;163:105243.
40. Loboda A, Damulewicz M, Pyza E, et al. Role of Nrf2/HO-1 system in development, oxidative stress response and diseases: an evolutionarily conserved mechanism. Cell Mol Life Sci. 2016;73:3221-47.
41. Lillig CH, Berndt C, Holmgren A. Glutaredoxin systems. Biochim Biophys Acta. 2008;1780:1304-17.
42. Lu J, Holmgren A. The thioredoxin antioxidant system. Free Radic Biol Med. 2014;66:75-87.
43. Dowling JK, Afzal R, Gearing LJ, et al. Mitochondrial arginase-2 is essential for IL-10 metabolic reprogramming of inflammatory macrophages. Nat Commun. 2021;12:1460.
44. Geiger R, Rieckmann JC, Wolf T, et al. L-Arginine Modulates T Cell Metabolism and Enhances

765 Survival and Anti-tumor Activity. Cell. 2016;167:829-42 e13.
766 45. Middleton SJ, Shorthouse M, Hunter JO. Increased nitric oxide synthesis in ulcerative colitis.
767 Lancet. 1993;341:465-6.
768 46. Rachmilewitz D, Stamler JS, Bachwich D, et al. Enhanced colonic nitric oxide generation and nitric
769 oxide synthase activity in ulcerative colitis and Crohn's disease. Gut. 1995;36:718-23.
770 47. Yasukawa K, Tokuda H, Tun X, et al. The detrimental effect of nitric oxide on tissue is associated
771 with inflammatory events in the vascular endothelium and neutrophils in mice with dextran
772 sodium sulfate-induced colitis. Free Radic Res. 2012;46:1427-36.
773